Ion impact crater asymmetry determines surface ripple orientation

M. Z. Hossain,[a] K. Das, J. B. Freund, and H. T. Johnson
Department of Mechanical Science and Engineering, University of Illinois at Urbana-Champaign, Urbana, Illinois 61801, USA

(Received 11 July 2011; accepted 12 September 2011; published online 12 October 2011)

Ion bombardment causes surface instabilities on a range of materials including metals, semiconductors, and insulators. However, the proposed mechanisms for these instabilities have yet to explain the rich range of nanometer-scale patterns that are observed experimentally. Here we show that smoothing balanced by impact angle dependent mass redistribution explains the atomistic origin of ripple formation and orientation, particularly angle dependent transitions between different orientations. A competition between the mass accumulated on the surface and the hole created on the surface determines the orientation of ripples. Results are consistent with experimental observations for a range of ions, ion energies, and targets. © *2011 American Institute of Physics*. [doi:10.1063/1.3650469]

The formation of nanometer-scale ripples on solid surfaces by ion bombardment is observed on semiconductors (Si, Ge),[1,2] metals (Cu, graphite),[3,4] and insulators (SiO_2),[5] and for different ion species including Ar,[1,6] Kr,[6] and Xe.[2,6] Ripples form either parallel or perpendicular to the beam direction and can change orientation if the impact angle changes. However, little is known about what atomistic mechanisms or features of individual ion impacts are linked to the formation of any particular ripple pattern, particularly its orientation. Here we consider Ar, Kr, and Xe ions with energies of 250 eV and 1500 eV impacting Si and Ge and study the growth and orientation of ripples. Our results suggest that ion induced surface redistribution, parameterized by moments of the craters formed by ion impacts, has a significant influence on ripple orientation.

According to the Bradley-Harper theory,[7] ripple formation is a surface instability with wavenumber q arising due to a q^2 dependent roughening mechanism, characterized by the so-called incident angle dependent sputtering coefficients Γ_x and Γ_y, and a q^4 dependent smoothing mechanism, with the relaxation coefficient B. The coefficients Γ_x and Γ_y are intended to model the spatial extent of the deposited energy and were initially based upon Sigmund's ellipsoidal energy deposition approximation.[8] Simulations[9–11] and experiments[12] both suggest that more mass is redistributed on the surface than is sputtered.

Using a moment-based description of mass redistribution effects, Norris *et al.*[11] explained the smoothing of surfaces under ion bombardment with off-normal incidence angles lower than 45°. Nevertheless, perpendicular ripples, as observed experimentally for angles higher than 80°, are not reproduced in their molecular dynamics (MD) based predictions. They speculate that this is related to the absence of explicit curvature dependence of crater functions.[11] Likewise because they find that the sign of Γ_y is always positive, its role on ripple formation or orientation is not reflected in their results or conclusions.

To better explain the atomistic processes of pattern formation over the range of ion energies and angles of incidence, we carry out highly accurate, statistically averaged molecular dynamics simulations and a crater-function multiscale analysis, based on the finite-amplitude modeling approach that was introduced by Kalyanasundaram *et al.*[10] We show that mass redistribution mediates ripple formation and orientation and that angle-dependent surface evolution can be explained by a combination of a standard q^4-dependent smoothing effect and a local-angle dependent mass redistribution. The evolution of surface patterns is simulated by numerically integrating the change in the height of a surface via[10]

$$h(\vec{r}, t+\Delta t) = h(\vec{r}, t) + \sum_{i=1}^{N} \Delta h_{ion}(\vec{r} - \vec{r}_0^{\,i}, \theta(\vec{r}_0^{\,i})) + \Delta h_{relaxation}, \tag{1}$$

where $\vec{r}$ is an arbitrary position on the surface, N is the number of random impacts over time Δt, r_0^i is the i^{th} random impact point, Δh_{ion} is the crater function representing the ensemble averaged mean change in surface height due to an impact, and $\Delta h_{relaxation}$ is the solution for the change in surface height due to surface relaxation over time Δt. As in the Bradley-Harper (BH) model, the relaxation is modeled as a fourth-order diffusion, $\partial_t h = -B\nabla^4 h$, which upon Fourier transformation has the solution

$$\hat{h}(\vec{q}, t+\Delta t) = \hat{h}(\vec{q}, t) e^{-B\Delta t(q_1{}^2+q_2{}^2)2}. \tag{2}$$

Here, $\Delta\hat{h}_{relaxation} = \hat{h}_{relaxation}(\vec{q}, t+\Delta t) - \hat{h}(\vec{q}, t)$ is the surface height change due to surface relaxation over Δt, and q_1 and q_2 are reciprocal-space coordinates. Surface relaxation, often modeled as we have done here with parameter B, has been used to model various mechanisms. It has been assumed to be thermally activated surface diffusion that involves atomic density of mobile species, temperature, surface energy, surface diffusivity, and atomic volume.[14,15] It has also been used to represent surface-tension driven viscous flow confined within a near-surface region around the point of impact.[16,17] The precise relaxation mechanism is unknown; our isotropic diffusion model, with B as a model parameter, is consistent with a range of potential phenomena. We take its effect to be isotropic, as it has typically been represented, so we can anticipate that its principal effect will be on ripple wavelength.

To associate ripple orientation with the geometric features of ion impacts, as quantified by their average crater

[a]Author to whom correspondence should be addressed. Electronic mail: zubaer@caltech.edu.

function, the redistribution of mass is analyzed by the low-order moments of the mean crater shape:

$$M_0 = \int h(x,y)dxdy = \text{SputterYield}, \tag{3a}$$

$$M_y = \int xh(x,y)dxdy, \tag{3b}$$

$$M_x = \int yh(x,y)dxdy, \tag{3c}$$

where x is the direction of the beam projected onto the mean surface plane and y is in this plane normal to the x-direction. The zeroth-order moment is proportional to sputter yield and is a scalar and therefore cannot be important for any directional effects such as ripple orientation. Ripple formation must therefore arise from first- and higher-order moments. M_x is zero due to symmetry of craters about the x-axis. We shall see that the behavior of the first-order moment about the y-axis, which represents the basic mass redistribution in the direction of the ion beam, is sufficient to explain changes in ripple orientation.

Anticipating this role of crater moments, particularly the effects of M_0, M_y, and B in the evolution equation, atomistic simulations are performed to compute realistic craters and their moments for a range of impact conditions involving 4 ion species (Ar, Kr, Xe, and Rn), 2 target materials (Si and Ge), 2 energies (250 eV and 1500 eV), and 9 angles of incidence (0°, 10°, 20°, 30°, 40°, 50°, 60°, 70°, and 80°). Example computed craters are shown in Fig. 1. The values of M_y for all of the craters are shown in Fig. 2. The details of the molecular dynamics simulations are reported in full detail elsewhere.[10]

For normal incidence, craters are always axisymmetric, and M_x and M_y are zero for any conditions, as shown in Fig. 2. On the other hand, off-normal impacts break the y-symmetry of the crater function as shown in Fig. 1. M_y is generally nonzero for off-normal incidence, except at the transition points where it changes its sign. For impact angles greater than 60°, rims are also significant in the lateral direction, as seen in Fig. 1 for the 80° crater plot. Hence, for larger angles the rim contribution to M_y is smaller than the hole contribution, making the net M_y negative.

We show here through computational results that the sign of M_y and $\partial_\theta M_y$ determines ripple orientation; ripples with q vector parallel to the beam direction are formed when $M_y > 0$ and $\partial_\theta M_y < 0$, and ripples with q vector perpendicular to the beam direction are formed when $M_y < 0$. The role of the sign of moments and their gradients can be explained by connecting moments to mass flux through linearized angle dependent coefficients,[11,18] which in the notation of BH yields

$$\Gamma_x(\theta) = \frac{d}{d\theta}[M_y(\theta)\cos\theta], \tag{4a}$$

$$\Gamma_y(\theta) = M_y(\theta)\cos\theta\cot\theta. \tag{4b}$$

The coefficients Γ_x or Γ_y contribute to surface evolution according to

$$\frac{\partial h}{\partial t} = \Gamma_x(\theta)\frac{\partial^2 h}{\partial x^2} + \Gamma_y(\theta)\frac{\partial^2 h}{\partial y^2} - B\nabla^4 h. \tag{4c}$$

When either Γ_x or Γ_y is negative, surface instability leads to the formation of ripples; for $\Gamma_x < 0$, parallel ripples are expected, and for $\Gamma_y < 0$, perpendicular ripples are expected. If both are positive, smoothing is anticipated to be dominant. On the other hand, if $\Gamma_y < 0$ and $\Gamma_x < 0$, then the conditions $|\Gamma_x| < |\Gamma_y|$ and $|\Gamma_y| > |\Gamma_x|$ would lead to parallel and perpendicular ripples, respectively. These linear predictions agree with finite-amplitude simulations we present with the MD craters as well as multiple experimental observations. For example, with the M_y values in Fig. 2, perpendicular ripples are predicted for 250 eV ion (Ar, Kr, or Xe) bombardment of Si or Ge, which is consistent with the experimental findings of perpendicular ripples for 250 eV Ar on Si at 10°,[13] 300 eV Kr on Si at 20°,[19] 500 eV Xe on Si at <30°,[6] and 500 eV Xe on Ge at <10°.[6] The computational results summarized in the moment diagram also predict perpendicular ripple formation at the highest angles of incidence, which agrees with the observation of perpendicular ripples for 1 keV Ar on Si,[13] 2 keV Kr on Si,[6] and 5 keV Xe on Si.[20] For Ar on Si at 250 eV and lower angles, the experimental observation of perpendicular ripples[13] is reported to be an experimental artifact. For these conditions, using our MD results in terms of Γ_x and Γ_y, formation of ripples is difficult to predict as Γ_x and Γ_y become comparable. However, our multiscale simulations show clearly that this condition leads to perpendicular ripples. In similar experimental conditions, Xe incident on Si and Ge forms perpendicular ripples.[6] Our results are also consistent with experimental observations of parallel ripples for Ar-Si at higher energies—500 eV (Fig. 1(d) in Ref. 6), 800 eV (Fig. 5(a) in Ref. 6), and 1200 eV (Fig. 5(b) in Ref. 6), all at 15° impact angle.

Additionally, the M_y-based criterion predicts a double transition (perpendicular-to-parallel-to-perpendicular as angle of incidence increases) for lower energy (<500 eV) ion bombardment of Si with Ar, Kr, and Xe, which agrees with the experimental evidence for Kr on Si (Ref. 19) and Xe on Si.[6] But as the impact energy increases, redistributive effects from the rim are more significant than redistributive hole effects even at lower angles, which suggests only a single orientation transition at higher energies. Also, for heavier ions at high incidence angles (~80°), the M_y contribution from the redistributed rim mass becomes stronger, which causes only parallel ripples to form, regardless of ion energy. Consequently, no perpendicular ripples were obtained in their MD predicted phase diagram.

To check the predictions based on the M_y criterion, full multiscale surface evolution simulations are performed with realistic MD-based craters obtained for Ar on Si at two

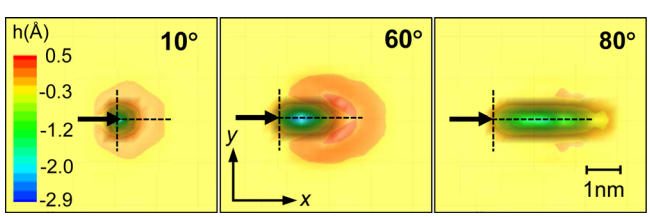

FIG. 1. (Color online) Effect of angle of incidence on crater shapes for 1500 eV Xe bombardment of Si. The beam direction is shown by the black arrow and the intersection of the dotted lines indicates the point of impact. The actual height of the crater rim (0.2 Å–1.0 Å) is much smaller than the lateral size (3.0–5.0 Å) of the crater. All of the craters are plotted using the same contour levels.

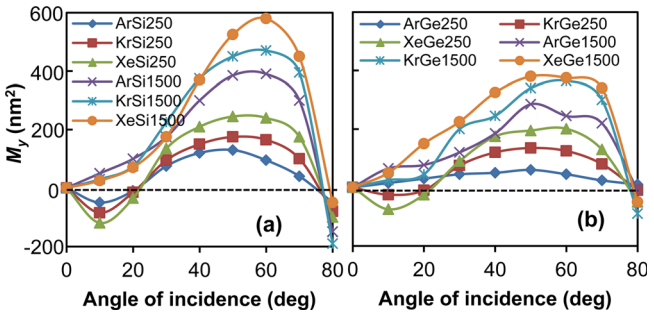

FIG. 2. (Color online) Variation of M_y for different species and energies for (a) Si and (b) Ge targets. For example, ArSi250 denotes 250 eV Ar ion bombardment of Si. The M_y value is zero for normal incidence and negative only for high angles or low angles with low ion energies.

different energies (250 eV and 1500 eV). A phase diagram containing these results as well as experimental results from the literature is shown in Fig. 3. The orientation predictions based on the M_y criterion are reproduced by the multiscale simulations based on realistic MD craters, and the results match most of the experimental observations. For Ar bombardment of Si at 250 eV from 30° to 70° incidence angle, our parallel ripples appear to be inconsistent with the experimentally observed flat surfaces. However, it should be noted that the amplitude of these ripples is only about 0.5 Å, which is essentially atomically flat. Indeed, a value for B can be chosen such that the experimentally observed smoothness is achieved.

Nonetheless, the experimental observation of both flat structures and ripple structures under the same impact conditions (Xe on Ge and Si at 2 keV at 20° angle of incidence) at different acceleration voltages[6] highlights the influence of an experimentally controllable parameter for tuning the wavelength of nanostructures. Consequently, flat and rippled structures both seem to appear at the same impact conditions. Thus, in terms of ripple orientation, the moment criterion and the MD computed results reproduce most of the experimental observations. Furthermore, the results indicate that the sign of

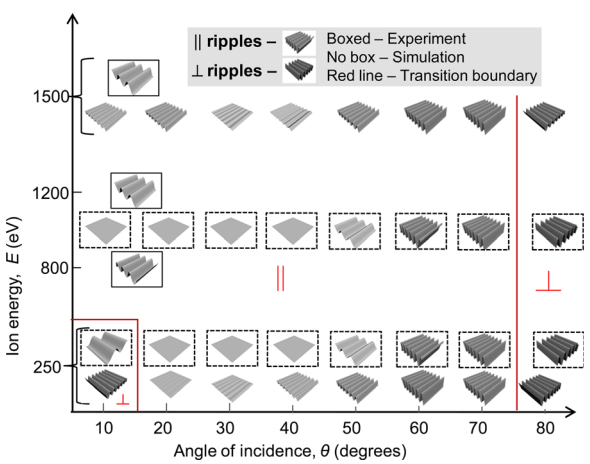

FIG. 3. (Color online) Ion energy and angle dependent surface morphology for Ar ion bombardment of Si. Each data "point" is represented by an oriented morphology image, with scaled wavelengths and amplitudes obtained from experimental and simulation results. Experimental morphologies are marked by rectangular boxes, where morphologies boxed with solid and dotted lines are taken from Ref. 6 and Ref. 13, respectively. The reference wavelength and amplitude are taken as 20 nm and 2 nm, respectively.

Γ_y, which is assumed to be always negative by Bradley and Harper, can be either positive or negative, and it plays an important role in explaining experimentally observed perpendicular ripples at beam angles lower than 30° for lower energy (500 eV) ion impacts. Our MD results and analysis also show that both Γ_y and Γ_x are important for surface morphology. Norris *et al.*[11] showed this in their surface transport model, but based on their MD results found Γ_y to be positive for all angles and Γ_x to be negative for all angles greater than 45°. Hence, they did not predict perpendicular ripples at large θ based on their MD results. Our results are consistent with the observed larger angle formation of perpendicular ripples for several ion-target combinations including Ar-Si.

It should be noted that the craters presented here were computed using a special procedure[21] to prevent mass conservation artifacts associated with crater computations using pre-impact and post-impact atomic positions or a probe atom method as is often done.[9–11] The differences in the MD-based phase diagrams reported in this work and in Ref. 11 are thought to derive from the method used in computing craters.

To summarize, we show that the sign of M_y and $\partial_\theta M_y$, as predicted based upon our MD results, together determine the orientation of the ripples observed. Local impact angle dependent mass redistribution and smoothing combined provide a comprehensive explanation for surface instability, formation of ripples, and their orientation and transitions as a function of angle of incidence.

[1]A. D. Brown, J. Erlebacher, W. L. Chan, and E. Chason, Phys. Rev. Lett. **95**, 056101 (2005).
[2]E. Chason, T. M. Mayer, B. K. Kellerman, D. T. McIlroy, and A. J. Howard, Phys. Rev. Lett. **72**, 3040 (1994).
[3]S. Rusponi, G. Costantini, C. Boragno, and U. Valbusa, Phys. Rev. Lett. **81**, 4184 (1998).
[4]P. F. A. Alkemade, Phys. Rev. Lett. **96**, 107602 (2006).
[5]S. Habenicht, W. Bolse, K. P. Lieb, K. Reimann, and U. Geyer, Phys. Rev. B **60**, R2200 (1999).
[6]B. Ziberi, M. Cornejo, F. Frost, and B. Rauschenbach, J. Phys. Condens. Matter **21**, 224003 (2009).
[7]R. M. Bradley and J. M. E. Harper, J. Vac. Sci. Technol. A **6**, 2390 (1988).
[8]P. Sigmund, J. Mater. Sci. **8**, 1545 (1973).
[9]N. Kalyanasundaram, M. Ghazisaeidi, J. B. Freund, and H. T. Johnson, Appl. Phys. Lett. **92**, 131909 (2008).
[10]N. Kalyanasundaram, J. B. Freund, and H. T. Johnson, J. Phys. Condens. Matter **21**, 224018 (2009).
[11]S. A. Norris, J. Samela, L. Bukonte, M. Backman, F. Djurabekova, K. Nordlund, C. S. Madi, M. P. Brenner, and M. J. Aziz, Nat. Commun. **2**, 276 (2011).
[12]C. S. Madi, E. Anzenberg, K. F. Ludwig, and M. J. Aziz, Phys. Rev. Lett. **106**, 066101 (2011).
[13]C. S. Madi, H. B. George, M. J. Aziz, J. Phys. Condens. Matter **21**, 224010 (2009).
[14]J. Erlebacher, M. J. Aziz, E. Chason, M. B. Sinclair, and J. A. Floro, Phys. Rev. Lett. **82**, 2330 (1999).
[15]M. A. Makeev and A.-L. Barabasi, Appl. Phys. Lett. **71**, 2800 (1997).
[16]C. C. Umbach, R. L. Headrick, and K. C. Chang, Phys. Rev. Lett. **87**, 246104 (2001).
[17]R. Cuerno, M. Castro, J. Munoz-Garica, R. Gago, and L. Vazques, Nucl. Instrum. Methods Phys. Res. **269**, 894 (2011).
[18]S. A. Norris, M. P. Brenner, and M. J. Aziz, J. Phys. Condens. Matter **21**, 224017 (2009).
[19]M. Cornejo, J. Vollner, and B. Ziberi, Adv. Struct. Mater. **10**, 69 (2011).
[20]K. Zhang, H. Hofsass, F. Rotter, M. Uhrmacher, C. Ronning, and J. Krauser, Surf. Coat. Technol. **203**, 2395 (2009).
[21]See supplementary material at http://dx.doi.org/10.1063/1.3650469 for local angle dependent mass distribution effects and crater computing methodology.